Implementation and Application of Density Functional Theory based Symmetry-Adapted Perturbation Theory for Dimers, Trimers and Molecular Crystals

Yi Xie

July 25, 2022

Noncovalent Interaction

- Phase transition, stability of crystal structure
- Drug binding, DNA/RNA/protein structure
- Many-body Expansion for the energy of complex system:

$$E = \sum_{A} E_A + \sum_{AB} E_{AB}^{\text{int},2} + \sum_{ABC} E_{ABC}^{\text{int},3} + \cdots$$

Intermolecular Energies

- Supermolecular approach

$$E_{AB}^{\text{int},2} = E_{AB} - E_A - E_B$$

$$E_{ABC}^{\text{int},3} = E_{ABC} - E_{AB} - E_{AC} - E_{BC} + E_A + E_B + E_C$$

- Symmetry-Adapted Perturbation Theory (SAPT)

$$E^{\text{int},2} = E_{\text{elst}}^{(1)} + E_{\text{exch}}^{(1)} + E_{\text{ind}}^{(2)} + E_{\text{exch-ind}}^{(2)} + E_{\text{disp}}^{(2)} + E_{\text{exch-disp}}^{(2)}$$

SAPT(DFT)

- Hamiltonian partitioning:

$$H = F_A + F_B + V_{AB} + W_A + W_B$$

$$H = K_A + K_B + V_{AB}$$

- "Uncoupled" sum-over-states approximation of $E^{(2)}_{\text{disp}}$ and in terms of frequency-dependent density susceptibility (FDDS):

$$\begin{aligned} E^{(2)}_{\text{disp,u}} &= -4 \sum_{ar\in A, bs\in B} \frac{\left|(ar|bs)\right|^2}{\epsilon^{rs}_{ab}} \\ &= -\frac{1}{2\pi}\int_0^\infty d\omega \int d\mathbf{r}_A d\mathbf{r}'_A d\mathbf{r}_B d\mathbf{r}'_B \\ &\quad \frac{1}{|\mathbf{r}_A - \mathbf{r}_B|} \frac{1}{|\mathbf{r}'_A - \mathbf{r}'_B|} \chi^A_0\left(\mathbf{r}_A, \mathbf{r}'_A|i\omega\right) \chi^B_0\left(\mathbf{r}_B, \mathbf{r}'_B|i\omega\right) \end{aligned}$$

Uncoupled $E_{\text{disp}}^{(2)}$

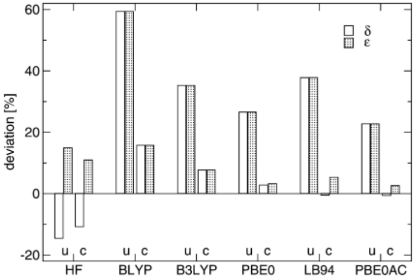

Fig. 2. Mean (δ) and mean absolute (ϵ) percental deviations of the uncoupled (u) and coupled (c) second-order dispersion energies from the MP2 results.

Mean (δ) and mean absolute (ϵ) percentage deviations of uncoupled (u) and coupled (c) $E_{\text{disp}}^{(2)}$ from SAPT2+ results.

A. Heßelmann and G. Jansen, Chem. Phys. Lett. **367**, 778 (2003).

Coupled $E^{(2)}_{\text{disp}}$

- Replacing uncoupled FDDS with coupled FDDS, solved from the coupled Kohn–Sham (CKS) TDDFT equation:

$$\chi = \chi_0 + \chi_0 \mathbf{S}^{-1}\mathbf{W}\left(\mathbf{S} - \chi_0 \mathbf{S}^{-1}\mathbf{W}\right)^{-1}\chi_0$$

- Exchange-correlation kernel term in $\mathbf{W}$ approximated by adiabatic local-density approximation (ALDA) kernel:

$$\begin{aligned} W_{PQ} &= \left(P|r_{12}^{-1}|Q\right) + \left(P|f_{\text{xc}}|Q\right) \\ &\approx \left(P|r_{12}^{-1}|Q\right) + \left(P|f_{\text{xc}}^{\text{ALDA}}|Q\right) \end{aligned}$$

M. Pitoňák and A. Hesselmann, J. Chem. Theory Comput. **6**, 168 (2010).

Hybrid Functional

- Local Hartree–Fock (LHF) approach
  - Computing LHF potential in each KS SCF iteration
  - $O(N^4)$ with very large constant factor
  - Different set of KS orbitals with smaller occupied–virtual gap
- Hybrid ALDA kernel
  - Mixing CHF and CKS equations to solve for FDDS
  - CKS involves integral of form $(ar|a'r')$, $O(N^4)$ with density fitting
  - CHF involves $(aa'|rr')$ and $(ar'|a'r)$, $O(N^5)$

Coupled $E^{(2)}_{\mathrm{exch-disp}}$

- Scaling from scaling uncoupled $E^{(2)}_{\mathrm{exch-disp}}$

$$\tilde{E}^{(2)}_{exch-disp,r} = E^{(2)}_{exch-disp,u} \cdot \frac{E^{(2)}_{disp,r}}{E^{(2)}_{disp,u}}$$

- Fixed scaling factor from fitting S22×5

$$\tilde{E}^{(2)}_{exch-disp,r} = \alpha \cdot E^{(2)}_{exch-disp,u} (\alpha = 0.686)$$

- Value of α above fitted from $E^{(2)}_{exch-disp,u}$ *with LHF orbitals*

A. Heßelmann and T. Korona, J. Chem. Phys. **141**, 094107 (2014).

S22 dimer set

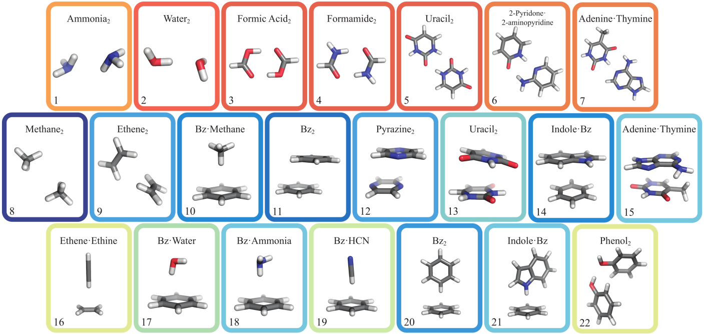

Coupled FDDS with hybrid kernel

- Recall coupled FDDS for pure ALDA kernel:

$$\chi = \chi_0 + \chi_0 \mathbf{S}^{-1}\mathbf{W}\left(\mathbf{S} - \chi_0 \mathbf{S}^{-1}\mathbf{W}\right)^{-1}\chi_0$$

- Coupled FDDS for hybird ALDA kernel, with $(aa'|rr')$ and $(ar'|a'r)$ contributions in χ_0' and $\mathbf{K}'$:

$$\chi = \chi_0' + \left(\chi_0' \mathbf{S}^{-1}\mathbf{W} + \mathbf{K}'\right)\left[\mathbf{S} - \left(\chi_0' \mathbf{S}^{-1}\mathbf{W} + \mathbf{K}'\right)\right]^{-1}\chi_0'$$

- Dispersion energy from integration over ω:

$$E^{(2)}_{\mathrm{disp,r}} = -\frac{1}{2\pi}\int_0^\infty d\omega \mathrm{Tr}\left(\mathbf{S}^{-1}\chi^A \mathbf{S}^{-1}\chi\right)$$

Refitting $E^{(2)}_{\mathrm{exch-disp,r}}$ for non-LHF orbitals

- LHF vs. non-LHF orbitals: Only affects uncoupled second-order terms like $E^{(2)}_{\mathrm{disp,u}}$ and $E^{(2)}_{\mathrm{exch-disp,u}}$
- Similar $E^{(2)}_{\mathrm{disp,r}}$ for LHF + pure ALDA vs. non-LHF + hybrid ALDA, expect the same for $E^{(2)}_{\mathrm{exch-disp,r}}$
- Can fit non-LHF $E^{(2)}_{\mathrm{disp,u}}$ to LHF + pure ALDA $E^{(2)}_{\mathrm{disp,r}}$:

$$\begin{aligned} E^{(2)}_{\mathrm{disp,r}}(hybrid) &\approx E^{(2)}_{\mathrm{disp,r}}(LHF) \\ &\approx \alpha \cdot E^{(2)}_{exch-disp,u}(non-LHF) \end{aligned}$$

- Fit for α using S22$\times$5 and test with S66$\times$8

SAPT terms: LHF vs non-LHF orbitals

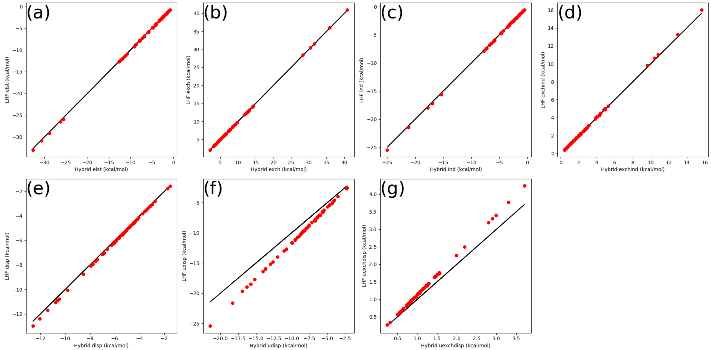

Hybrid vs. LHF values in kcal/mol for each term for S66 data set: (a) $E^{(1)}_{\text{elst}}$, (b) $E^{(1)}_{\text{exch}}$, (c) $E^{(2)}_{\text{ind}}$, (d) $E^{(2)}_{exch-ind}$, (e) $E^{(2)}_{disp,r}$, (f) $E^{(2)}_{disp,u}$, (g) $E^{(2)}_{exch-disp,u}$

Fitting Results

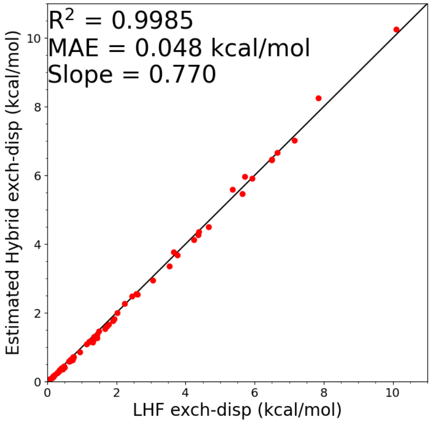

Idea of SAPT(DFT)

- SAPT energy in orders of interaction and fluctuation potentials; n denotes order in V and k, l for W_A, W_B

$$H = F_A + F_B + V + W_A + W_B$$

$$E_{int} = \sum_{n=1}^{\infty} \sum_{k=0}^{\infty} \sum_{l=0}^{\infty} \left(E_{pol}^{(nkl)} + E_{exch}^{(nkl)} \right)$$

- SAPT0: $n = 2, k = l = 0$, no intramonomer correlation, $O(N^5)$ cost
- Many-body SAPT: $k + l \geq 2$, $O(N^6)$ or higher cost
- SAPT(DFT): Use Kohn-Sham operator $K_{A,B}$ instead of Fock operator $F_{A,B}$, $O(N^5)$ cost
- Primitive SAPT(DFT) works well on 1st-order terms, but not 2nd-order terms (especially dispersion). Needs orbital response for these terms

Coupled Dispersion Energy

- Uncoupled dispersion energy in terms of frequency-dependent density susceptibility (FDDS):

$$
\begin{aligned}
E^{(2)}_{disp,u} &= -4 \sum_{ia\in A, jb\in B} \frac{\left|(ia|jb)\right|^2}{\epsilon^{ab}_{ij}} \\
&= -\frac{1}{2\pi}\int_0^\infty d\omega \int d\mathbf{r}_A d\mathbf{r}'_A d\mathbf{r}_B d\mathbf{r}'_B \\
&\quad \frac{1}{|\mathbf{r}_A - \mathbf{r}_B|}\frac{1}{|\mathbf{r}'_A - \mathbf{r}'_B|}\chi^A_0\left(\mathbf{r}_A, \mathbf{r}'_A|i\omega\right)\chi^B_0\left(\mathbf{r}_B, \mathbf{r}'_B|i\omega\right)
\end{aligned}
$$

- Kohn-Sham DFT constructs a fictitious system of non-interacting particles, which reproduces the density and energy of the real electronic system
- Kohn-Sham FDDS does not reflect the correct response properties of the electronic system

Dispersion Term

- Coupled FDDS from solving TDDFT equations[0]:

$$\chi = \chi_0 + \chi_0 \mathbf{S}^{-1}\mathbf{W}\left(\mathbf{S} - \chi_0 \mathbf{S}^{-1}\mathbf{W}\right)^{-1}\chi_0$$

- $\mathbf{S}$ and $\mathbf{W}$ corresponds to Coulomb metric and xc kernel
- Pure ALDA kernel good for pure GGA functional, but not for hybrid functional
- Exact exchange in v_{xc} $\rightarrow$ increased ϵ_{ij}^{ab} $\rightarrow$ decreased $E_{disp}^{(2)}$

$$E_{disp,u}^{(2)} = -4 \sum_{ia\in A, jb\in B} \frac{\left|(ia|jb)\right|^2}{\epsilon_{ij}^{ab}}$$

- Hybrid ALDA kernel to compensate, or localized HF (LHF) exchange to avoid increase in ϵ_{ij}^{ab}
- Reformulating solution of hybrid TDDFT equations[1] in density-fitting basis on next slide

[0] M. Pitoňák and A. Hesselmann, J. Chem. Theory Comput. **6**, 168 (2010).

Coupled FDDS with hybrid kernel

$$\chi = \chi_0' + \left(\chi_0'\mathbf{S}^{-1}\mathbf{W} + \mathbf{K}'\right)\left[\mathbf{S} - \left(\chi_0'\mathbf{S}^{-1}\mathbf{W} + \mathbf{K}'\right)\right]^{-1}\chi_0'$$

$$\mathbf{K}' = \left[-\xi\mathbf{K}_1\left(\lambda d\right) - \xi\mathbf{K}_2\left(\lambda d\right) + \xi^2\mathbf{K}_{21}\left(\lambda\right)\right]\left(\mathbf{R}^T\right)^{-1}\mathbf{S}$$

$$[\mathbf{K}_1(\lambda d)]_{PQ} = (P|ar)\lambda_{ar}d_{ar}[(aa'|rr') + (ar'|a'r)](a'r'|\mathbf{Q}|Q)$$

$$[\mathbf{K}_2(\lambda d)]_{PQ} = (P|ar)\lambda_{ar}d_{ar}[(aa'|rr') - (ar'|a'r)](a'r'|\mathbf{Q}|Q)$$

$$\begin{aligned}[\mathbf{K}_{21}(\lambda)]_{PQ} \quad &= \quad (P|ar)\lambda_{ar}[(aa''|rr'') - (ar''|a''r)] \\ &\quad\quad [(a'a''|r'r'') - (a'r''|a''r')](a'r'|\mathbf{Q}|Q)\end{aligned}$$

$$[\mathbf{K}_2'(\lambda)]_{PQ} = (P|ar)\lambda_{ar}[(aa'|rr') - (ar'|a'r)](a'r'|Q)$$

$$\chi_0' = \chi_0 - \xi\mathbf{K}_2\left(\lambda\right)$$

$$(ar|Q) = (ar|\mathbf{Q}|P)(P|\mathbf{R}|Q)$$

Exchange-Dispersion Term

- Explicit coupled exchange-dispersion not trivial to implement; currently working on this
- Estimate from scaling uncoupled exchange-dispersion; Scale with ratio in dispersion term or with pre-fitted (with S22×5) fixed factor

$$\tilde{E}^{(2)}_{exch-disp,r} = E^{(2)}_{exch-disp,u} \cdot \frac{E^{(2)}_{disp,r}}{E^{(2)}_{disp,u}}$$

$$\tilde{E}^{(2)}_{exch-disp,r} = \alpha \cdot E^{(2)}_{exch-disp,u} (\alpha = 0.686)$$

- The value above is fitted from $E^{(2)}_{exch-disp,u}$ with LHF orbitals
- Non-LHF orbitals have greater o-v gaps and smaller $E^{(2)}_{disp,u}$, needs to re-fit with non-LHF results

Equation for $E^{(2)}_{disp}$

- Coupled Kohn-Sham (CKS) FDDS reflects correct response properties of electrons
- $O(N^5)$ scaling is limited to forming $\mathbf{K}_1$, $\mathbf{K}_2$, $\mathbf{K}_{21}$ and $\mathbf{K}'_2$. These quantities are frequency-dependent, but could store frequency-independent intermediates from the $O(N^5)$ contractions on disk, and the frequency-dependent contractions are only $O(N^4)$
- $E^{(2)}_{disp}$ from coupled FDDS: (Integration is approximated by Gauss-Legendre quadrature)

$$
\begin{aligned}
E^{(2)}_{disp,r} = & -\frac{1}{2\pi}\int_0^\infty d\omega \int d\mathbf{r}_A d\mathbf{r}'_A d\mathbf{r}_B d\mathbf{r}'_B \\
& \frac{1}{|\mathbf{r}_A - \mathbf{r}_B|}\frac{1}{|\mathbf{r}'_A - \mathbf{r}'_B|}\chi^A\left(\mathbf{r}_A, \mathbf{r}'_A|i\omega\right)\chi^B\left(\mathbf{r}_B, \mathbf{r}'_B|i\omega\right)
\end{aligned}
$$

LHF vs non-LHF orbitals

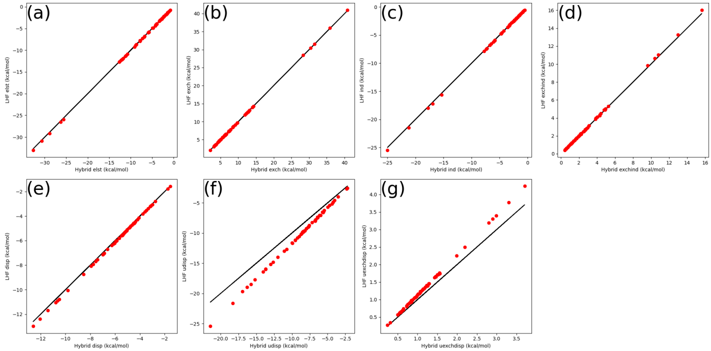

Hybrid vs. LHF values in kcal/mol for each term for S66 data set: (a) $E^{(1)}_{elst}$, (b) $E^{(1)}_{exch}$, (c) $E^{(2)}_{ind}$, (d) $E^{(2)}_{exch-ind}$, (e) $E^{(2)}_{disp,r}$, (f) $E^{(2)}_{disp,u}$, (g) $E^{(2)}_{exch-disp,u}$

Exchange-Dispersion Refitting

- Need to fit the uncoupled $E^{(2)}_{exch-disp,r}$ with non-LHF orbitals on the coupled LHF orbital values (implemented in Molpro)
- Assuming coupled LHF and non-LHF orbital $E^{(2)}_{exch-disp,r}$ from the behavior of $E^{(2)}_{disp,r}$
- Exchange-related components depend heavily on distance between monomers, sets like S22×5 and S66×8 would be preferred (S22/S66 with various non-equilibrium intermolecular distances)
- Determine the scaling factor with S22×5, validate with S66×8

S22 dimer set

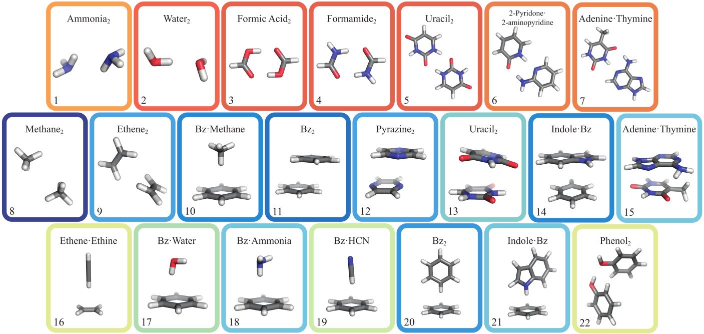

S22×5 Fitting Results

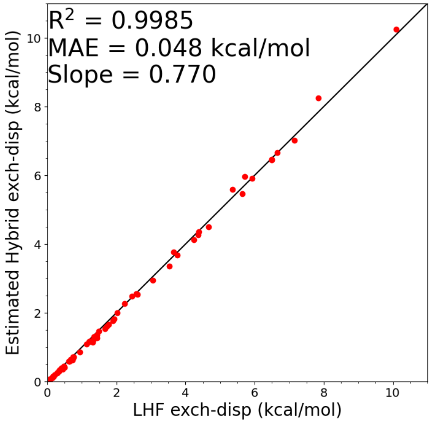

S66×8 Validating Results

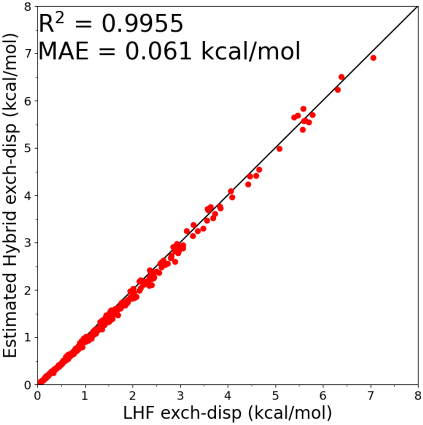

Termwise results

- Compared the SAPT(DFT)/aug-cc-pVTZ results of our code to SAPT(CCSD)/aug-cc-pVTZ results from Korona S2[2]
- Also comparing the results for S66 with SAPT2+3(CCD)δMP2/aug-cc-pVTZ as reference. Also added SAPT0/aug-cc-pVDZ, SAPT2+/aug-cc-pVDZ and SAPT2+(3)δMP2/aug-cc-pVTZ into comparison as side-reference.
- Errors of each system with respect to reference shown as vertical lines
- Mean absolute error (MAE) and mean unsigned relative error (MURE) listed for S2. MAE indicated by black box in the diagram
- Color scheme for S66 systems: Hydrogen-bonded (HB, red), mixed-influence (MX, green), dispersion-dominated (DD, blue)

[2] T. Korona, Mol. Phys. **111**, 3705 (2013).

Korona S2 Results

Method	MAE	MURE
Electrostatics		
SAPT(DFT) hybrid	0.112	2.39
SAPT(DFT) LHF	0.114	3.68
SAPT0	0.520	8.61
Exchange		
SAPT(DFT) hybrid	0.251	3.38
SAPT(DFT) LHF	0.258	3.09
SAPT0	1.757	12.88
Induction		
SAPT(DFT) hybrid	0.148	2.79
SAPT(DFT) LHF	0.192	2.97
SAPT0	1.993	16.83
Exchange-Induction		
SAPT(DFT) hybrid	0.144	4.03
SAPT(DFT) LHF	0.165	4.76
SAPT0	1.551	26.80

Error Distribution

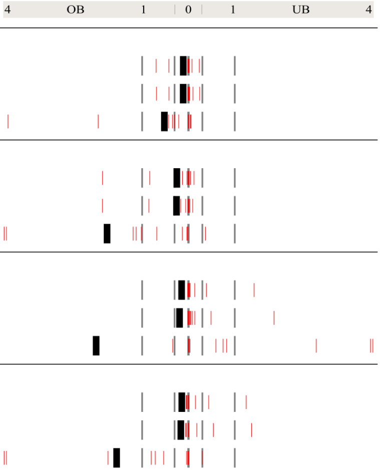

Korona S2 Results

Method	MAE	MURE	Error Distribution
Dispersion			
SAPT(DFT) hybrid	0.175	3.68	
SAPT(DFT) LHF	0.141	2.77	
SAPT(DFT) non-hybrid	0.326	9.58	
SAPT0	0.811	24.86	
Exchange-Dispersion			
SAPT(DFT) hybrid	0.062	12.47	
SAPT(DFT) LHF	0.039	3.25	
SAPT0	0.265	36.11	
Total			
SAPT(DFT) hybrid	0.155	4.98	
SAPT(DFT) LHF	0.189	4.17	
SAPT(DFT) hon-hybrid	0.244	10.64	
SAPT0	1.237	19.63	

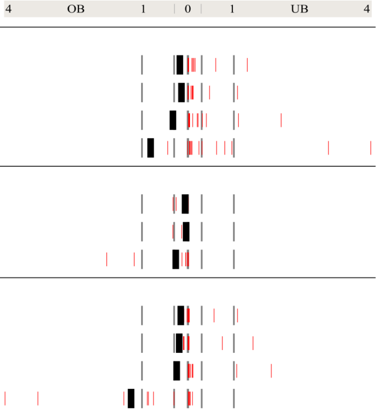

Georgia Tech

S66 Results

Method	Total	HB	MX	DD
Electrostatics				
SAPT(DFT) hybrid	0.374	0.556	0.177	0.311
SAPT(DFT) LHF	0.423	0.666	0.196	0.319
SAPT0	0.613	1.034	0.439	0.297
SAPT2+	0.236	0.270	0.136	0.263
SAPT2+(3)δMP2	0.000	0.000	0.000	0.000
Exchange				
SAPT(DFT) hybrid	0.886	1.127	0.426	0.926
SAPT(DFT) LHF	0.886	1.121	0.431	0.928
SAPT0	0.675	0.942	0.263	0.658
SAPT2+	0.337	0.467	0.222	0.277
SAPT2+(3)δMP2	0.000	0.000	0.000	0.000
Induction				
SAPT(DFT) hybrid	0.211	0.201	0.212	0.220
SAPT(DFT) LHF	0.224	0.223	0.223	0.225
SAPT0	0.241	0.200	0.261	0.271
SAPT2+	0.327	0.384	0.250	0.318
SAPT2+(3)δMP2	0.152	0.179	0.121	0.145

Error Distribution

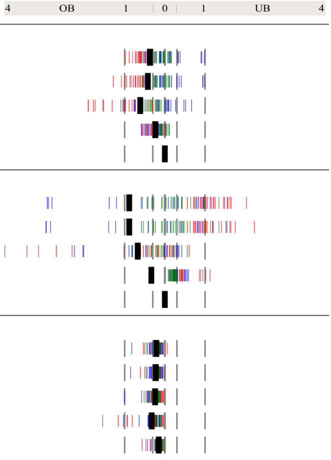

S66 Results

Method	Total	HB	MX	DD	Error Distribution
Dispersion					
SAPT(DFT) hybrid	0.370	0.260	0.219	0.573	
SAPT(DFT) LHF	0.308	0.200	0.173	0.499	
SAPT(DFT) non-hybrid	0.635	0.581	0.419	0.822	
SAPT0	0.443	0.862	0.162	0.195	
SAPT2+	0.235	0.397	0.169	0.115	
SAPT2+(3)δMP2	0.093	0.129	0.056	0.080	
Total					
SAPT(DFT) hybrid	0.334	0.588	0.107	0.217	
SAPT(DFT) LHF	0.234	0.382	0.046	0.199	
SAPT(DFT) non-hybrid	0.604	0.955	0.389	0.385	
SAPT0	0.990	1.197	0.692	0.965	
SAPT2+	0.230	0.235	0.138	0.280	
SAPT2+(3)δMP2	0.105	0.056	0.082	0.169	

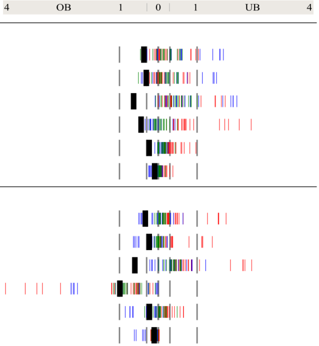

Timing Performance

- Analyzing breakdown wall times for subroutines in SAPT(DFT) for a few systems with 500–3000 basis functions
- Using Intel Core i7-6800K processor with 6 cores for Watson-Crick adenine-thymine complex and RDX dimer
- Using Intel Core i9-10980XE processor with 18 cores for C_{60}–buckycatcher ($N_{bf} = 3012$), completed entire calculation in 4.03 days
- Contribution of $O(N^5)$ dispersion terms not dominant for smaller systems
- Cost of SCF (HF/DFT) calculations and induction terms are usually non-negligible

Timing Systems

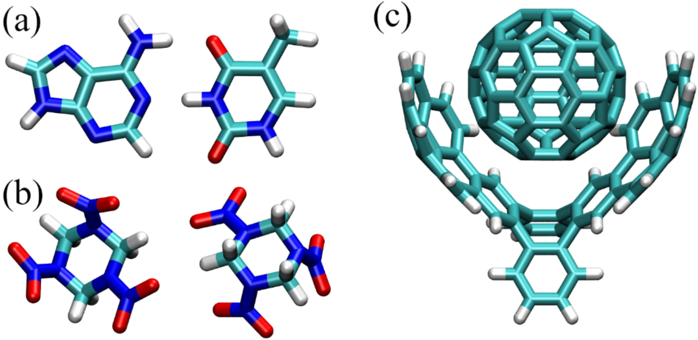

Dimer systems for timing: (a) Watson-Crick adenine-thymine complex, (b) RDX dimer, (c) C_{60}–buckycather complex.

Watson-Crick Adenine-Thymine

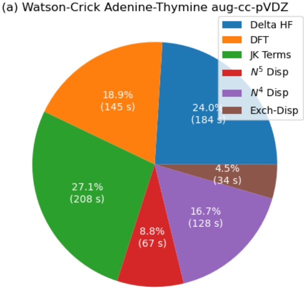

$N_{bf} = 536$

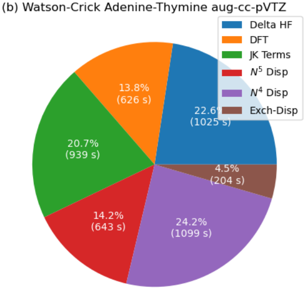

$N_{bf} = 1127$

RDX Dimer

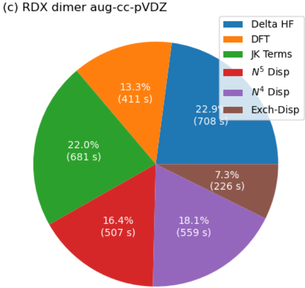

$N_{bf} = 798$

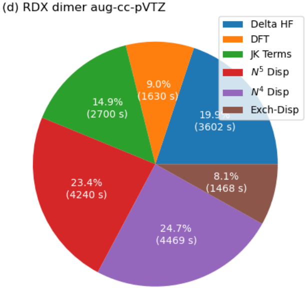

$N_{bf} = 1656$

Comparison with LHF Approach

- Comparison of subrountine wall times between hyybrid xc kernel approach implemented in Psi4 1.4 and LHF approach implemented in Molpro 2019.2
- Some subroutines does not exist or not included by default in the Molpro DFT-SAPT program

Subroutine	Psi4 hybrid time (h)	Molpro LHF time (h)
Delta HF	0.96	N/A
DFT	0.45	2.29
xc kernel	0.08	4.17
$O(N^5)$ objects formation	2.35	N/A
$E_{disp}^{(2)}$ time integration	0.37	3.59
$E_{exch-disp}^{(2)}$	0.41	1.99
Total	5.03	12.80

C_{60}–Buckycatcher Complex

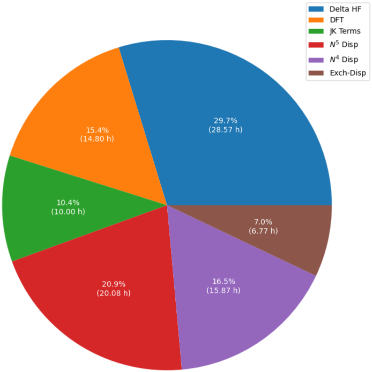

$N_{bf} = 3012$

3B-69 Benchmark Set

- Benchmark set for 3-body interaction energies[3]
- 69 trimers extracted from 23 different molecular crystal structures (3 each)
- Used focal point approach to obtain CCSD(T) (and other wavefunction method) energies

$$E = E^{\mathrm{HF}}(\mathrm{aQZ}) + \Delta\mathrm{E}^{\mathrm{MP2}}(\mathrm{aTZ/aQZ}) + \Delta\mathrm{E}^{\mathrm{CCSD(T)}}(\mathrm{aDZ})$$

- Assessing accuracy for various wavefunction and DFT methods
- Authors recommended MP2.5 and SCS-MI-CCSD, both $O(N^6)$
- We will extend this work to assess the performance of MP2+FDDS (dispersion) for 3B-69 systems

[3] J. Řezáč et al., J. Chem. Theory Comput. **11**, 3065 (2015).

3B-69 Wavefunctional Methods

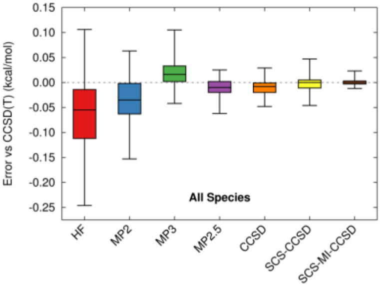

- MP2.5 and SCS-MI-CCSD exhibits best cost performance, as in the two-body case
- MP2.5, MP3: Non-iterative $O(N^6)$
- CCSD and variants: Iterative $O(N^6)$

3B-69 DFT Methods

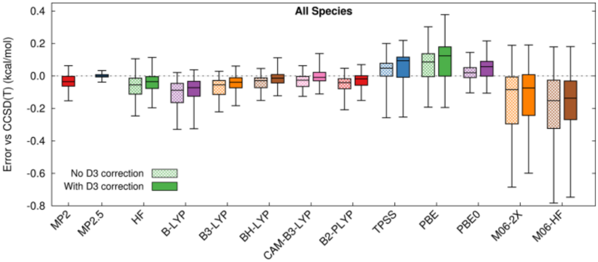

- DFT-D3 accuracies comparable to MP2 at the best, in contrast to the two-body case where DFT-D3 models significantly outperform MP2
- Delocalization error leads to errors in many-body polarization and exchange

Three-Body FDDS Dispersion

- Three-body dispersion energy in terms of FDDS, analogous to the two-body dispersion:

$$
\begin{aligned}
E^{(3)}_{disp,r} \quad = \quad & -\frac{1}{\pi}\int_0^\infty d\omega \int d\mathbf{r}_A d\mathbf{r}'_A d\mathbf{r}_B d\mathbf{r}'_B d\mathbf{r}_C d\mathbf{r}'_C \\
& \frac{1}{|\mathbf{r}_A - \mathbf{r}_B|}\frac{1}{|\mathbf{r}'_A - \mathbf{r}_C|}\frac{1}{|\mathbf{r}'_B - \mathbf{r}'_C|} \\
& \chi^A\left(\mathbf{r}_A, \mathbf{r}'_A|i\omega\right)\chi^B\left(\mathbf{r}_B, \mathbf{r}'_B|i\omega\right)\chi^C\left(\mathbf{r}_B, \mathbf{r}'_B|i\omega\right)
\end{aligned}
$$

- Transform from position space into density-fitting auxiliary basis space:

$$
E^{(3)}_{disp,r} = \int_0^\infty d\omega \, \mathrm{Tr}\left(\mathbf{S}^{-1}\boldsymbol{\chi}^A\mathbf{S}^{-1}\boldsymbol{\chi}^B\mathbf{S}^{-1}\boldsymbol{\chi}^C\right)
$$

New Set from X23

- Aiming to construct a "three-body version" of S22$\times$5/S66$\times$8 to investigate three-body interaction for trimers with different intermolecular distances and alignments
- Sampling trimer geometries from X23 crystal structures
- Distance: Geometric mean and mininum of 3 pairwise closest contact distances
- Alignment: Angles of the COM triangle; mainly looking at the greatest angle

Research Plan

- Check if MP2+FDDS (dispersion) is a good model for three-body non-additive interaction energy
- If not, compare FDDS dispersion with estimated three-body dispersion energy from $E^{\mathrm{CCSD(T)}} - E^{\mathrm{MP2}}$
- Investigate the dependence of three-body dispersion energies on intermolecular distances and alignments, and the difference between FDDS dispersion and $E^{\mathrm{CCSD(T)}} - E^{\mathrm{MP2}}$ for different trimer geometries
- Choosing dispersion dominated systems (such as benzene) in X23 to avoid zero dispersion energies at longer distance.

3B-69 Initial Test: Systems

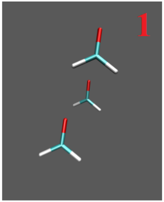

formaldehyde b

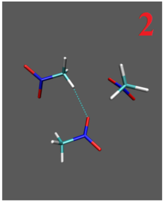

nitromethane a

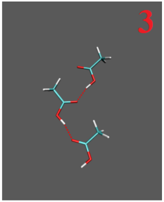

acetic acid b

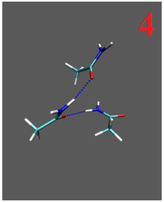

acetamide a

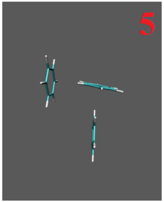

benzene c

3B-69 Initial Test: Results

- Total three-body non-additive interaction energies in kcal/mol
- CCSD(T) and MP2.5 interaction energies from focus point approach

System	CCSD(T)	MP2+ FDDS/aDZ	MP2+ FDDS/aTZ	MP2	MP2.5
1	0.181	0.207	0.210	0.161	0.179
2	-0.122	-0.069	-0.065	-0.178	-0.143
3	-0.922	-0.905	-0.904	-0.937	-0.913
4	-0.089	-0.003	-0.003	-0.239	-0.151
5	-0.027	0.002	0.003	-0.061	-0.023

3B-69 Initial Test: Results

- Comparison of estimated 3-body dispersion energies
- ΔCCSD(T) corresponds to dispersion energy estimated by $E^{\mathrm{CCSD(T)}} - E^{\mathrm{MP2}}$

System	ΔCCSD(T)	FDDS/aDZ	FDDS/aTZ
1	0.020	0.046	0.049
2	0.056	0.109	0.113
3	0.015	0.032	0.033
4	0.150	0.236	0.242
5	0.034	0.063	0.064

3B-69 Three-Body Dispersion: ΔMP2.5

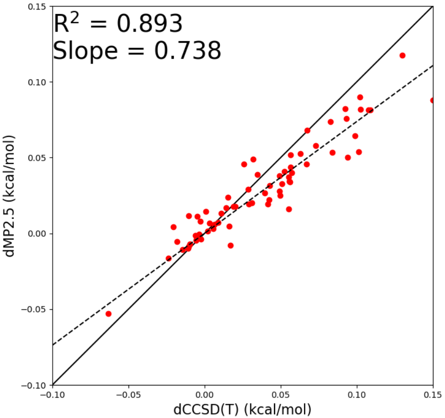

3B-69 Three-Body Dispersion: FDDS

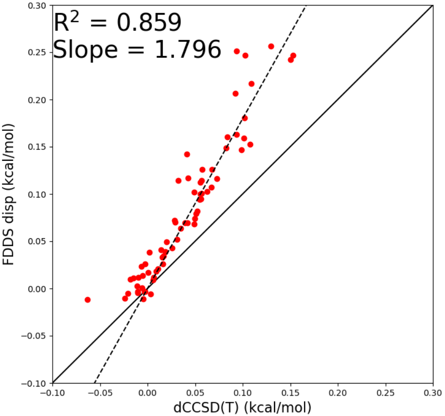

Crystalline Benzene 3-Body Dispersion

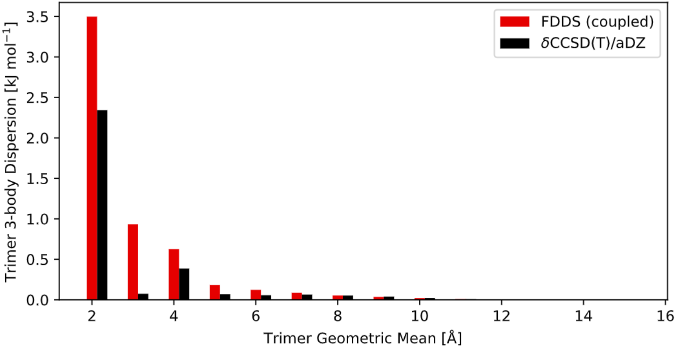

Crystalline Benzene 3-Body Dispersion

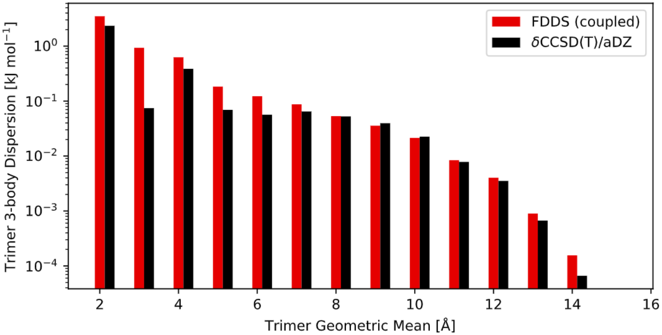

Acknowledgment

Thesis advisor:

Dr. C. David Sherrill

Thesis committee members:

Dr. Jesse G. McDaniel

Dr. Thomas M. Orlando

Dr. Edmond Chow

Dr. Joshua S. Kretchmer

Special thanks for implementing 3-body FDDS dispersion and providing data for crystalline benzene:

Zachary L. Glick